Tuning Thermoelectric Properties of Bi2Ca2Co2Oy through K doping and Laser Floating Zone processing

Can Özçelik
Iskenderun Technical University: Iskenderun Teknik Universitesi
Tolga Depci (tdepci@gmail.com)
Iskenderun Technical University: Iskenderun Teknik Universitesi
Mehmet Gürsul
Cukurova University: Cukurova Universitesi
Gizem Çetin
Cukurova University: Cukurova Universitesi
Bekir Özçelik
Cukurova University: Cukurova Universitesi
Miguel A. Torres
Universidad de Zaragoza
Maria A. Madre
University of Zaragoza: Universidad de Zaragoza
Andres Sotelo
University of Zaragoza: Universidad de Zaragoza

Research Article

Keywords: Thermoelectric oxides, Seebeck Coefficient, Resistivity, Power Factor

Posted Date: June 11th, 2021

DOI: https://doi.org/10.21203/rs.3.rs-607259/v1

Tuning Thermoelectric Properties of $Bi_2Ca_2Co_2O_y$ through K doping and Laser Floating Zone processing

C. Özçelik[1], T. Depci[1*], M. Gürsul[2], G. Çetin[2], B. Özçelik[2], M. A. Torres[3], M. A. Madre[3], A. Sotelo[3]

[1]Iskenderun Technical University, Institute of Engineering and Sciences, Hatay, Turkey

[2]Department of Physics, Faculty of Sciences and Letters, Çukurova University, 01330 Adana, (Turkey).

[3]INMA (CSIC-Universidad de Zaragoza), C/María de Luna 3, 50018-Zaragoza (Spain).

Abstract

In the present study, thermoelectric $Bi_2Ca_{2-x}K_xCo_2O_y$ ceramic materials (x=0.0, 0.05, 0.075, 0.10, and 0.125) in different forms (called bulk, as-grown and annealed fibers) have been manufactured via a classical solid-state method and textured using the laser floating zone (LFZ) technique. The identification and characteristics of undoped and doped samples were determined by X-ray diffraction (XRD) and scanning electron microscopy (SEM). The XRD patterns of all samples have shown great similarity, and the major peaks can be assigned to the $Bi_2Sr_2Co_2O_y$ thermoelectric phase, independently of the processing technique and K-doping. SEM-EDS have indicated the randomly oriented plate like grains of different sizes in bulk sample, evolving to longer and well-oriented grain structure through K-doping and LFZ. Because of the incongruent melting properties of compound, the high number of secondary phases formed in the as-grown samples. In order to reduce it, an annealing and K-doping process have been applied. The microstructural evolution is reflected on the electrical properties, and the lowest resistivity values are found in the annealed K-doped fibers. Seebeck coefficient is positive in all cases, pointing out to p-type conduction mechanism. These modifications led to PF values up to 0.162 mW/K^2m, obtained in 0.10 K-doped annealed fibers at 650 ^oC.

Keywords: Thermoelectric oxides; Seebeck Coefficient; Resistivity; Power Factor;

Corresponding author: Tolga Depci
e-mail: tdepci@gmail.com

1. Introduction

Thermoelectric (TE) materials are quite popular owing their capability of converting wasted heat energy to useful electric power using Seebeck effect [1]. The efficiency of such conversion is evaluated through the dimensionless figure of merit, ZT, defined as $TS^2/\rho\kappa$, where T is the absolute temperature, S the Seebeck coefficient, κ the thermal conductivity, and ρ the electrical resistivity. It seems that promising TE materials must possess high Seebeck coefficient, low thermal conductivity and electrical resistivity, and high working temperatures. TE materials comprise a large number of families involving binary phases of Bi-Te, Co-Sb, Pb-Te, silicides, as Mg-Si, or Mn-Si, and oxides [2]. Among these types, ceramic CoO-based TE materials are quite attractive owing to their abundance in the earth crust, high working temperatures, and relatively lower toxicity and costs than the other families [3,4]. The first discovered CoO-based material, Na_xCoO_2, exhibited large thermoelectric power breaking the general belief that oxides had poor thermoelectric properties [5]. This study led to the discovery of new layered cobaltites such as Ca-Co-O [6], Bi-Ca-Co-O [7], and Bi-Sr-Co-O [8]. From various crystallographic studies, it has been found that the crystal structures of CoO-based (TE) materials can be described through a monoclinic structure, which is composed of an alternate stacking of two different layers, namely CdI_2-type CoO_2 conductive layer and rock salt (RS) $Bi_2X_2O_4$ (X=Ca, Sr and Ba) insulating one. These two layers have common *a*- and *c*-axis lattice parameters with different *b*-axis length, which causes a misfit along the *b*-direction [7,9,10]. Layered cobaltites are known to have a large crystallographic anisotropy, which is reflected in an anisotropic behavior of electrical properties. For example, Seebeck coefficient, S, may be tuned up through variations of misfit factor or the oxidation state of cations in the RS substructure [11]. These variations can be carried out through different material preparation procedures, as the alignment of plate-like grains by texturing techniques [12-14], or chemical processes as substituting different elements into the matrix [15-19].

The aim of the present study is to determine the effect of microstructure modification on the thermoelectric properties of $Bi_2Ca_2Co_2O_y$ ceramic materials prepared by solid state method and processed using different techniques. In addition, the influence of partial Ca by K substitution on the different processed materials will be evaluated.

2. Experimental Procedure

The $Bi_2Ca_{2-x}K_xCo_2O_y$ (x = 0.0, 0.05, 0.075, 0.10 and 0.125) ceramic precursors were obtained from commercial Bi_2O_3 (Panreac, 98 + %), $CaCO_3$ (98.5 %, Panreac), K_2CO_3 (Panreac, 98 + %), and Co_2O_3 (Aldrich, 98 + %) powders. They were weighed in stoichiometric proportions, and milled in a ball-mill for 30 minutes at 300 rpm in acetone medium. Then, the mixture was dried using infrared irradiation and manually re-grinded to produce fine powders, which were subsequently calcined twice at 750 and 800 ºC for 12 hours to decompose the metallic carbonates. Part of these powders has been pressed into pellets under 400 MPa applied pressure, and sintered at 810 ºC for 24 h with a final furnace cooling. The obtained materials after this process will be called bulk samples throughout the text. The other part of the powders were pressed into cylinders (around 3 mm diameter and 100 mm length) by means of isostatic pressure under 200 MPa, followed by texturing in a LFZ system, using previously described conditions [20]. The samples produced through the LFZ treatment will be called as-grown fibers. Moreover, due to the incongruent melting shown by this compound some of the as-grown fibers were annealed in an oven for 24 hours at 800°C with a final furnace cooling in order to increase the amount of thermoelectric phase [21]. The samples obtained after this process will be named as annealed fibers throughout the text.

Powder X-ray diffraction (XRD) has been used to determine the phases present in the samples, using a Rigaku D/max-B system between 20 and 40º. The microstructural studies have been made on longitudinal polished sections of all samples using secondary electrons in a field emission scanning electron microscope (FESEM, Zeiss Merlin), while EDS analysis has been used to determine the qualitative composition of the different phases. Electrical resistivity and Seebeck coefficient have been simultaneously determined using a LSR-3 device (Linseis GmbH) under He atmosphere and temperatures between 50 and 650 ºC. Moreover, these data have been used to calculate the thermoelectric power factor (PF, defined as S^2/ρ).

3. Results and discussion

XRD patterns of $Bi_2Ca_{2-x}K_xCo_2O_y$ bulk, as-grown, and annealed fibers are given in Fig. 1. From these figures, it is clear that most of the observed peaks correspond to $Bi_2Ca_2Co_2O_y$ thermoelectric phase, independently of the processing technique and K-substitution in agreement with previous studies [22]. Further, there is no significant peaks shift with K substitution, while the absence of K-based secondary phases could indicate its successful

incorporation into the main matrix in all cases. On the other hand, some secondary phases are observed in all as-grown samples and in undoped bulk sample and annealed fibers. The larger content of secondary phases in as-grown samples, when compared to the other two types of samples prepared in this work, is related to the incongruent melting resulting from LFZ process and observed in similar systems [20,23]. Consequently, it can be easily deduced that annealing process at 800 °C for 12 h, drastically decreases the amount of these secondary phases as observed in the XRD patterns of the annealed fibers. In addition, secondary phases content is further decreased in bulk samples and annealed fibers with K-substitution.

In order to evaluate grain orientation in the different samples, Lotgering factor (LF), defined as $LF = (P-P_0)/(1-P_0)$, where P is the sum of the peak intensities of preferred orientation, and P_0 is the P of samples with randomly-oriented grains [24-25], has been calculated for all samples, and presented in Table 1. When observing the effect of K-doping on the different samples, bulk samples and annealed fibers clearly show higher grain orientation when K content is increased. On the other hand, as-grown fibers do not show a clear tendency, as it is decreased up to 0.075 K, increasing for higher content. This fact can be explained by the large amount of secondary phases in these samples, when compared to the other ones, probably producing important modifications in the peaks intensities due to overlapping of peaks of secondary and thermoelectric phases.

SEM technique and EDS analysis are used to investigate surface morphology and determine the elemental composition of the different phases. The structural evolution of samples with K content for bulk samples, and as grown, and annealed fibers, is displayed in Fig. 2, for x=0 and 0.075K. From these micrographs it can be observed that all samples present three contrasts. EDS has allowed associating each contrast to different phases. Grey contrast (#1) corresponds to the thermoelectric $Bi_2Ca_2Co_2O_y$ phase, white contrast (#2) to Bi/Ca oxide in different Bi:Ca proportions, and black contrast (#3) to Co oxide. Moreover, no K-based secondary phase has been detected in any of the samples, in accordance with the XRD data. When comparing undoped specimens to the doped ones, it is evident that K-substitution increases density in bulk samples, eliminating the typical porosity produced through the solid state method [26], while slightly increases grain orientation in as-grown and annealed fibers. When considering the secondary phases content, as-grown fibers show the highest content, as previously mentioned, due to the incongruent melting observed in these compounds. However, annealing procedure drastically decreases black contrast (Co oxide, #3) and, in lower content, white one (Bi-Ca oxides, #2). In any case, the sizes of these Bi-Ca oxide phases are much larger than the observed in the bulk samples, but they display some

orientation along the growth direction. All these observations fit well with the previously discussed XRD data. In addition, K^+ incorporation into the system further increases grain orientation most probably due to the decrease of melting point of the system associated to the formation of a Bi_2O_3-K_2CO_3 eutectic which decreases the thermal radial gradient during the LFZ processing, as observed in similar systems [27].

Fig. 3 displays the electrical resistivity measurements, as a function of temperature, for all samples. As it can be seen from the figure, the behavior of the *ρ(T)* curves is quite different, depending on the processing route. All as-grown fibers exhibit semiconducting-like behavior ($d\rho/dT<0$) independently of K-concentration. On the other hand, bulk samples and annealed fibers display a metallic-like ($d\rho/dT>0$) one, except for the undoped ones, which exhibit semiconductor-like behavior in the whole measured temperature range in annealed fibers, while for the bulk sample it is semiconductor-like up to 500 ºC, and metallic-like one above this temperature. In all cases, electrical resistivity values are decreased by K-doping, regardless of the processing technique. Since K^+ substitution for Ca^{2+} reduces the total charge in the rock-salt layers and induces the promotion of Co^{3+} to Co^{4+} in the conduction layer, increasing the charge carrier concentration which leads to lower resistivity values [19]. On the other hand, the high resistivity observed in as-grown fibers is due to the high amount of secondary phases, together with a large content of oxygen vacancies, as previously reported [28]. Furthermore, the drastic decrease of electrical resistivity in annealed fibers, when compared to the as-grown ones, is due to the formation of thermoelectric phase from the secondary ones, the enhancement of grain orientation, and the decrease of oxygen vacancies which increase charge carrier concentration. This evolution can be easily observed in Table 1, where the resistivity values of all samples at 650 ºC are displayed. The minimum values at 650 ºC have been determined in 0.075K annealed fibers (26.4 mΩ cm), which are same order of the Pb-substituted textured materials with much higher cationic substitution and prepared through solution method (~ 30 mΩ cm) [14], and much lower than the reported in sintered materials (~ 70 mΩ cm) [7]. On the other hand, the values are still far from the reported in single crystals at room temperature (6 mΩ cm) [29].

The electrical conduction mechanism in misfit-layered $Bi_2Ca_{2-x}K_xCo_2O_y$ is based on the small polaron hopping model [30-32] where resistivity is given as:

$$\rho\,(T) = \left(\frac{T}{Anea^2}\right)\exp\left(\frac{E_a}{k_B T}\right) \qquad (1)$$

where A is the pre-exponential term related to the scattering mechanism, n the carrier concentration, e the elementary charge, a the intersite distance of the hopping, k_B the Boltzman constant, T the absolute temperature, and E_a the activation energy. The linear fits of ln(ρ/T) versus 1000/T presented in Fig. 4 (for clarity for x=0 and 0.075K are presented) indicate that small polaron hopping transport model is a good description of the conduction mechanism of these samples. In order to calculate E_a, the slopes of fits in Fig. 4 are used, and the results are presented in Table 1. According to the table, it can be observed that E_a values for undoped samples are higher than the calculated for K-substituted samples, independently of the processing method. The decrease in the E_a values is another explanation for the observed decrease in the electrical resistivity, as discussed above [31].

Seebeck coefficient variation with respect to temperature for all $Bi_2Ca_{2-x}K_xCo_2O_y$ samples is given in Fig. 5. All Seebeck coefficients are positive in the whole measured temperature range which is an indication of p-type conduction mechanism. When comparing the values determined in the different samples, it is clear that as-grown fibers display the highest Seebeck coefficient at any temperature and composition. This effect is associated to a higher amount of oxygen vacancies in these fibers, as reported in previous works [33]. The maximum value of this coefficient at room temperature has been determined in 0.05K as-grown fibers (around 225 μV/K), much higher than the reported in single crystals (~ 150 μV/K) [34]. A theoretical model of thermopower (or Seebeck coefficient) in cobalt oxides was proposed by Koshibae et al. [35], as follows:

$$S = -\frac{k_B}{|e|} ln\left(\frac{1}{6}\frac{x}{1-x}\right) \quad (2)$$

where k_B is the Boltzmann constant, e the charge of electron, and x the concentration of Co^{+4} ions in the conduction band. By using this formula and the Seebeck values measured at 650ºC (see Table-1), the fraction of Co^{+4} in each sample has been calculated and presented in Table 1. From these values, it can be observed that all doped samples have higher Co^{+4} concentration, in agreement with the previous discussion in the electrical resistivity section. According to Koshibae's model, there is no S dependence with temperature when measuring it at high temperatures. However, this model is not realistic enough as it is ignoring the peculiar splitting of the t_{2g} levels in the CoO_2 layer [36]. Hence, it is well known that, in real conditions, Seebeck coefficient values are influenced by temperature. Consequently, the highest S values for each sample have been determined at 650 ºC, independently of processing

method. The maximum values in annealed samples at 650 ºC (about 225 μV/K) are lower than the measured in as-grown samples at the same temperature (~ 285 μV/K). In any case, they are higher than the reported in sintered materials (~ 150 μV/K) [37], or produced through solution methods (~ 215 μV/K) [38], but lower than the measured in hot-pressed ceramics (~ 250 μV/K) [39].

The estimation of thermoelectric performances of all samples has been made using power factor (PF) values, obtained from Seebeck coefficient and resistivity data, and represented in Fig. 6. From these graphs it can be seen that PF values of all K-substituted samples are higher than the obtained in the undoped ones due to the drastic decrease of electrical resistivity induced by K-substitution. Besides, in spite of the high amount of secondary phases, as-grown fibers display only slightly lower PF values than the sintered samples. This effect clearly point out to a higher influence of grain orientation and connectivity than the amount of secondary phases. Consequently, the highest PF values have been determined in annealed fibers, which combine the highest grain orientation among all samples, with a decrease of the secondary phases content, when compared to the as-grown ones. The maximum PF values at 650 ºC, presented in Table-1, has been determined in 0.10K annealed fibers (0.162 mW/K^2m), which is around eight times higher than the reported in sintered materials (~ 0.02 mW/K^2m) [37], slightly higher than the obtained in samples prepared through solution methods (~ 0.09 mW/K^2m) [38], but still lower than the reported in hot-pressed materials (~ 0.25 mW/K^2m) [39]. It should be highlighted that these last samples combine high grain orientation, high density, low amount of secondary phases, and probably optimal oxygen content in the thermoelectric phase.

4. Conclusions

In this study, $Bi_2Ca_{2-x}K_xCo_2O_y$ (x=0, 0.05, 0.075, 0.10, and 0.125) bulk samples, as-grown and annealed fibers have been prepared by solid-state reaction, LFZ processing, and LFZ processing followed by annealing, respectively. XRD graphs showed that most of the observed peaks corresponded to the $Bi_2Ca_2Co_2Oy$ thermoelectric phase, showing the independent character of the processing technique and K-substitution. From SEM-EDS investigations, it has been determined that K-substitution reduced the amount of porosity and Co oxide secondary phase in bulk samples, and improved grain alignment in annealed fibers. These structural and microstructural modifications were reflected in the electrical resistivity values, which were lower in K-substituted specimens than in undoped ones, regardless of the

processing route. On the other hand, Seebeck coefficient values agreed with the electrical resistivity ones, being higher when the measured electrical resistivity was higher due to the decrease of Co^{4+} concentration in undoped samples, when compared to the K-substituted ones. The best thermoelectric performances, evaluated using PF, were obtained in annealed fibers, which show the best combination of density, grain orientation, secondary phases content, and charge carrier concentration. However, these high PF values were still lower than the obtained in hot-pressed materials, probably due to the difficult oxygen diffusion through the fibers during annealing process due to their high density, resulting in higher oxygen vacancies than usual in sintered or hot-pressed materials.

Acknowledgements

The results used in the framework of this study are related to the MSc thesis of C. Özçelik. M. A. Torres, M. A. Madre, and A. Sotelo acknowledge MINECO-FEDER (MAT2017-82183-C3-1-R, and Gobierno de Aragón-FEDER (Research Group T54-20R) for funding. Authors acknowledge the use of Servicio General de Apoyo a la Investigación-SAI, Universidad de Zaragoza.

References

[1] D. Champier, Thermoelectric generators: A review of applications, Energy Convers. Manage. 140 (2017) 167–181.

[2] M. H. Elsheikh, D. A. Shnawah, M. F. M. Sabri, S. B. M. Said, M. H. Hassan, M. B. A. Bashir, M. Mohamad, A review on thermoelectric renewable energy: Principle parameters that affect their performance, Renew. Sust. Energ. Rev. 30 (2014) 337–355.

[3] S. LeBlanc, Thermoelectric generators: Linking material properties and systems engineering for waste heat recovery applications, Sust. Mater. Technol. 1-2 (2014) 26–35.

[4] J. He, Y. Liu, R. Funahashi, Oxide thermoelectrics: The challenges, progress, and outlook, J. Mater. Res. 26 (2011) 1762–1772.

[5] I. Terasaki, Y. Sasago, K. Uchinokura, Large thermoelectric power in $NaCo_2O_4$ single crystals, Phys. Rev. B 56 (1997) 12685–12687.

[6] S. Li, R. Funahashi, I. Matsubara, K. Ueno, H. Yamada, High temperature thermoelectric properties of oxide $Ca_9Co_{12}O_{28}$, J. Mater. Chem. 9 (1999) 1659–1660.

[7] A. Maignan, S. Hébert, M. Hervieu, C. Michel, D. Pelloquin, D. Khomskii, Magnetoresistance and magnetothermopower properties of Bi/Ca/Co/O and Bi(Pb)/Ca/Co/O misfit layer cobaltites, J. Phys. Condens. Matter 15 (2003) 2711–2723.

[8] R. Funahashi, I. Matsubara, S. Sodeoka, Thermoelectric properties of $Bi_2Sr_2Co_2O_x$ polycrystalline materials, Appl. Phys. Lett. 76 (2000) 2385–2387.

[9] H. Itahara, C. Xia, J. Sugiyama, T. Tani, Fabrication of textured thermoelectric layered cobaltites with various rock salt-type layers by using β-$Co(OH)_2$ platelets as reactive templates, J. Mater. Chem. 14 (2004) 61–66.

[10] X. G. Luo, Y. C. Jing, H. Chen, X. H. Chen, Intergrowth and thermoelectric properties in the Bi–Ca–Co–O system, J. Cryst. Growth 308 (2007) 309–313.

[11] A. Maignan, D. Pelloquin, S. Hebert, Y. Klein, M. Hervieu, Thermoelectric power in misfit cobaltites ceramics: Optimization by chemical substitutions. Bol. Soc. Esp. Ceram. V. 45 (2006) 122–125.

[12] H. Wang, X. Sun, X. Yan, D. Huo, X. Li, J.-G. Li, X. Ding, Fabrication and thermoelectric properties of highly textured $Ca_9Co_{12}O_{28}$ ceramic, J. Alloy. Compd. 582 (2014) 294–298.

[13] Sh. Rasekh, G. Constantinescu, M. A. Torres, M. A. Madre, J. C. Diez, A. Sotelo, Growth rate effect on microstructure and thermoelectric properties of melt grown $Bi_2Ba_2Co_2O_x$ textured ceramics, Adv. Appl. Ceram. 111 (2012) 490–494.

[14] Sh. Rasekh, M. A. Madre, J. C. Diez, E. Guilmeau, S. Marinel, A. Sotelo, Effect of Pb substitution on the thermoelectrical properties of textured $Bi_2Ca_2Co_{1.7}O_y$ ceramics prepared by a polymer solution method, Bol. Soc. Esp. Ceram. V. 49 (2010) 371–376.

[15] G. Çetin Karakaya, B. Özçelik, M. A. Torres, M. A. Madre, A. Sotelo, Effect of Na-doping on thermoelectric and magnetic performances of textured $Bi_2Sr_2Co_2O_y$ ceramics, J. Eur. Ceram. Soc. 38 (2018) 515–520

[16] S. Butt S, Y. C. Liu, J. L. Lan, K. Shehzad, B. Zhan, Y. Lin, C. W. Nan, High-temperature thermoelectric properties of La and Fe co-doped Ca-Co-O misfit-layered cobaltites consolidated by spark plasma sintering, J. Alloy. Compd. 588 (2014) 277–283.

[17] H. S. Hao, Q. L. He, L. M. Zhao, Thermoelectric Properties of Cu-substituted $Bi_2Ca_2Co_2O_y$ Misfit Oxides, Adv. Mater. Res. 284-286 (2011) 2263–2267.

[18] G. Çetin Karakaya, B. Özçelik, O. Nane, A. Sotelo, Sh. Rasekh, M. A. Torres, M. A. Madre, Improvement of $Bi_2Sr_2Co_2O_y$ thermoelectric performances by Na doping, J. Electroceram. 40 (2018) 11–15

[19] G. Çetin Karakaya, B. Özçelik, , M. A. Torres, M. A. Madre, A. Sotelo, Effects of K substitution on thermoelectric and magnetic properties of $Bi_2Sr_2Co_2O_y$ ceramic, J. Mater. Sci. Mater. Electron. 28 (2017) 12652–12659.

[20] Sh. Rasekh, F. M. Costa, N. M. Ferreira, M. A. Torres, M. A. Madre, J. C. Diez, A. Sotelo, Use of laser technology to produce high thermoelectric performances in $Bi_2Sr_2Co_{1.8}O_x$, Mater. Des. 75 (2015) 143–148.

[21] D. Flahaut, J. Allouche, A. Sotelo, Sh. Rasekh, M. A. Torres, M. A. Madre, J. C. Diez, Role of Ag in textured-annealed $Bi_2Ca_2Co_{1.7}O_x$ thermoelectric ceramic, Acta Mater. 102 (2016) 273–283.

[22] Sh. Rasekh, M. A. Madre, A. Sotelo, E. Guilmeau, S. Marinel, J. C. Diez, Effect of synthetic methods on the thermoelectrical properties of textured $Bi_2Ca_2Co_{1.7}O_x$ ceramics, Bol. Soc. Esp. Ceram. V. 49, 89–94 (2010).

[23] B. Özçelik, G. Çetin, M. Gürsul, M.A. Madre, A. Sotelo,A study on thermoelectric performance and magnetic properties of Ti-doped $Bi_2Sr_2Co_{1.8}O_y$ ceramic materials, Mater. Chem. Phys. 256 (2020) 12370.

[24] F. K. Lotgering, Topotactical reactions with ferrimagnetic oxides having hexagonal crystal structures—I, J. Inorg. Nucl. Chem. 9 (1959) 113–123.

[25] R. Furushima, S. Tanaka, Z. Kato, K. Uematsu, Orientation distribution–Lotgering factor relationship in a polycrystalline material—as an example of bismuth titanate prepared by a magnetic field, J. Ceram. Soc. Jpn. 118 (2010) 921–926.

[26] Sh. Rasekh, G. Constantinescu, M. A. Madre, M. A. Torres, J. C. Diez, A. Sotelo, Processing effects on the thermoelectric properties of $Bi_2Ca_2Co_{1.7}O_x$ ceramics, Bol. Soc. Esp. Ceram. V. 53 (2014) 207–212.

[27] B. Ozcelik, G. Cetin, M. Gursul, M. A. Madre, A. Sotelo, S. Adachi, Y. Takano, Low temperature thermoelectric properties of K-substituted $Bi_2Sr_2Co_2O_y$ ceramics prepared via laser floating zone technique, J. Eur. Ceram. Soc. 39 (2019) 3082–3087.

[28] A. Sotelo, E. Guilmeau, M. A. Madre, S. Marinel, S. Lemmonier, J. C. Diez, $Bi_2Ca_2Co_{1.7}O_x$ thermoelectric ceramics textured by laser floating zone method, Bol. Soc. Esp. Ceram. V. 47 (2008) 225–228.

[29] N. Sun, S. T. Dong, B. B. Zhang, Y. B. Chen, J. Zhou, S. T. Zhang, Z. B. Gu, S. H. Yao, Y. F. Chen, Intrinsically modified thermoelectric performance of alkaline-earth isovalently substituted $[Bi_2AE_2O_4][CoO_2]_y$ single crystals, J. Appl. Phys. 114 (2013) 043705.

[30] A. J. Bosman, H. J. V. Daal, Small-polaron versus band conduction in some transition-metal oxides, Adv. Phys. 19 (1970) 1–117.

[31] N. Prasoetsopha, S. Pinitsoontorn, T. Kamwanna, V. Amornkitbamrung, K. Kurosaki, Y. Ohishi, H. Muta, S. Yamanaka, The effect of Cr substitution on the structure and properties of misfit-layered $Ca_3Co_{4-x}Cr_xO_{9+\delta}$ thermoelectric oxides, J. Alloy. Compd. 588 (2014) 199–205.

[32] U. Hira, N. Pryds, F. Sher, Thermoelectric Properties of Dual Doped $Bi_2Sr_2Co_2O_y$-Based Ceramics, J. Electron. Mater. 48 (2019) 4618–4626.

[33] G. Constantinescu, Sh. Rasekh, M. A. Torres, M. A. Madre, J. C. Diez, A. Sotelo, Enhancement of the high-temperature thermoelectric performance of $Bi_2Ba_2Co_2O_x$ ceramics, Scr. Mater. 68 (2012) 75–78.

[34] E. Guilmeau, M. Pollet, D. Grebille, D. Chateigner, B. Vertruyen, R. Cloots, R. Funahashi, B. Ouladiaff, Neutron diffraction texture analysis and thermoelectric properties of BiCaCoO misfit compounds, Mater. Res. Bull. 43 (2008) 394–400.

[35] W. Koshibae, K. Tsutsui, S. Maekawa, Thermopower in cobalt oxides, Phys. Rev. B. 62 (2000) 6869–6872.

[36] L. H. Yin, R. Ang, L. J. Li, B. C. Zhao, Y. K. Fu, X. B. Zhu, Z. R. Yang, W. H. Song, Y. P. Sun, Thermoelectric properties of sol–gel derived cobaltite $Bi_2Ca_{2.4}Co_2O_y$, Physica B 406 (2011) 2914–2918.

[37] A. I. Klyndyuk, N. S. Krasutskaya, A. A. Khort, Synthesis and Properties of Ceramics Based on a Layered Bismuth Calcium Cobaltite, Inorg. Mater. 54 (2018) 509–514.

[38] A. Sotelo, Sh. Rasekh, M. A. Madre, E. Guilmeau, S. Marinel, J. C. Diez, Solution-based synthesis routes to thermoelectric $Bi_2Ca_2Co_{1.7}O_x$, J. Eur. Ceram. Soc. 31 (2011) 1763–1769.

[39] E. Guilmeau, M. Mikami, R. Funahashi, D. Chateigner, Synthesis and thermoelectric properties of $Bi_{2.5}Ca_{2.5}Co_2O_x$ layered cobaltites, J. Mater. Res. 20 (2005) 1002–1008.

Figure Captions:

Figure-1. XRD results for all $BiCa_{2-x}K_xCo_2O_y$ samples, (a) bulk, (b) as-grown, (c) annealed fibers.

Figure-2. SEM micrographs and EDS analysis performed in representative $BiCa_{2-x}K_xCo_2O_y$ samples, (a) bulk, (b) as-grown, (c) annealed fibers.

Figure-3. Electrical resistivity variation with temperature for all $BiCa_{2-x}K_xCo_2O_y$ samples, (a) bulk, (b) as-grown, (c) annealed fibers.

Figure-4. ln(ρ/T) versus 1000/T graph of representative $BiCa_{2-x}K_xCo_2O_y$ samples, for x=0 and 0.075.

Figure-5. Seebeck coefficient variation with temperature for all $BiCa_{2-x}K_xCo_2O_y$ samples, (a) bulk, (b) as-grown, (c) annealed fibers.

Figure-6. Power factor evolution with temperature for all $BiCa_{2-x}K_xCo_2O_y$ samples, (a) bulk, (b) as-grown, (c) annealed fibers.

Table:

Table-1. Lotgering factors, resistivity values at 650 ^oC, Activation energies, Seebeck coefficents at 650 ^oC, fraction of Co^{+4}, Power factors at 650 ^oC

Figures

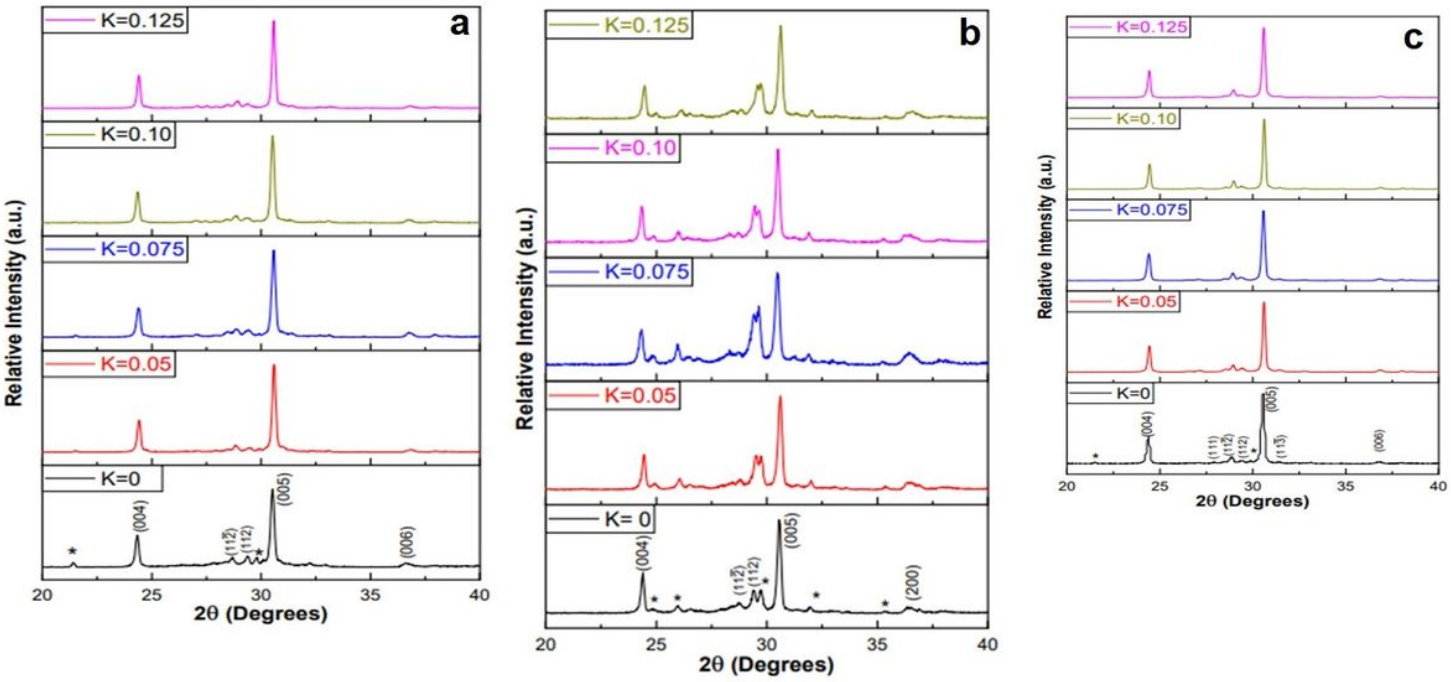

Figure 1

XRD results for all BiCa2-xKxCo2Oy samples, (a) bulk, (b) as-grown, (c) annealed fibers.

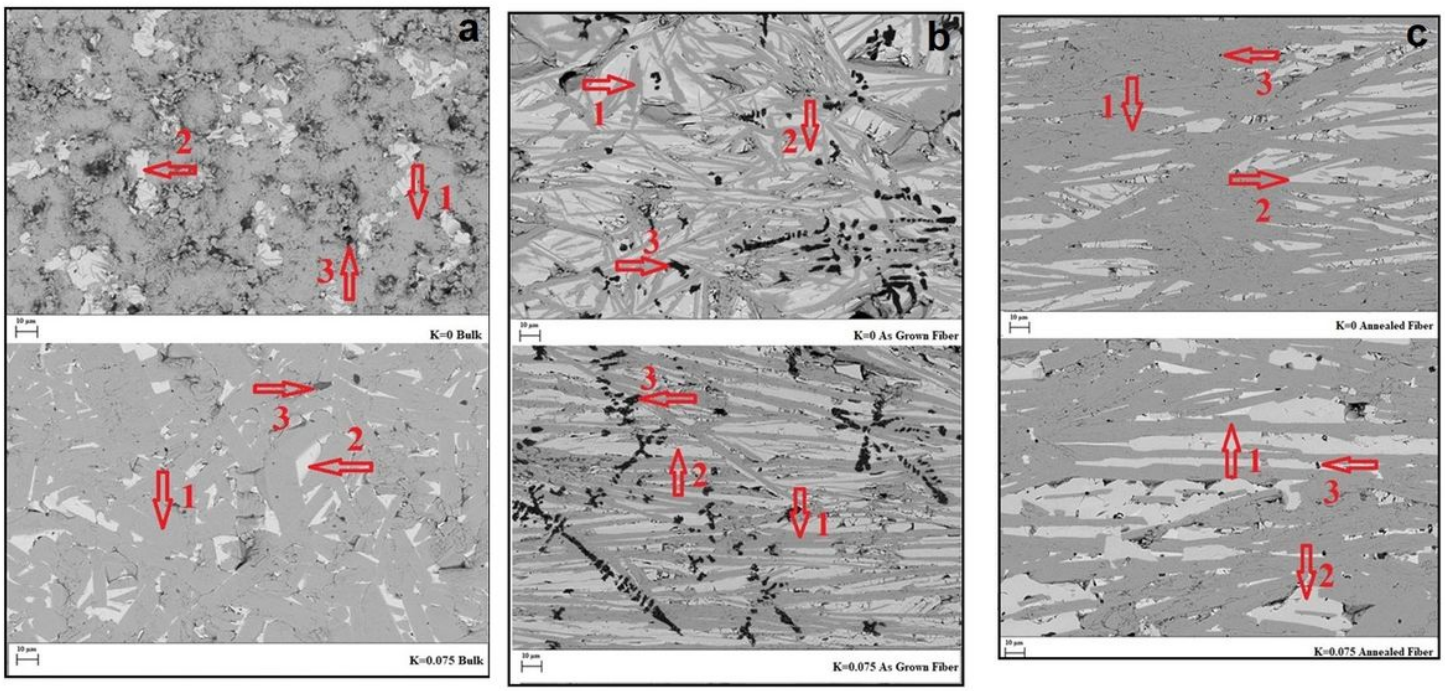

Figure 2

SEM micrographs and EDS analysis performed in representative BiCa2-xKxCo2Oy samples, (a) bulk, (b) as-grown, (c) annealed fibers.

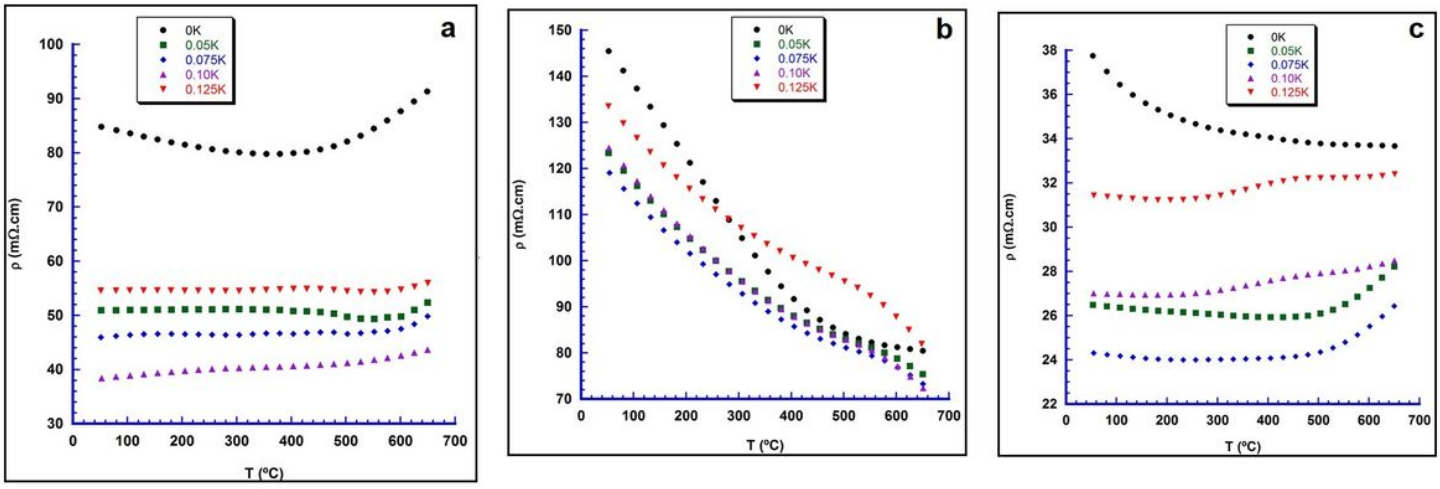

Figure 3

Electrical resistivity variation with temperature for all BiCa2-xKxCo2Oy samples, (a) bulk, (b) as-grown, (c) annealed fibers.

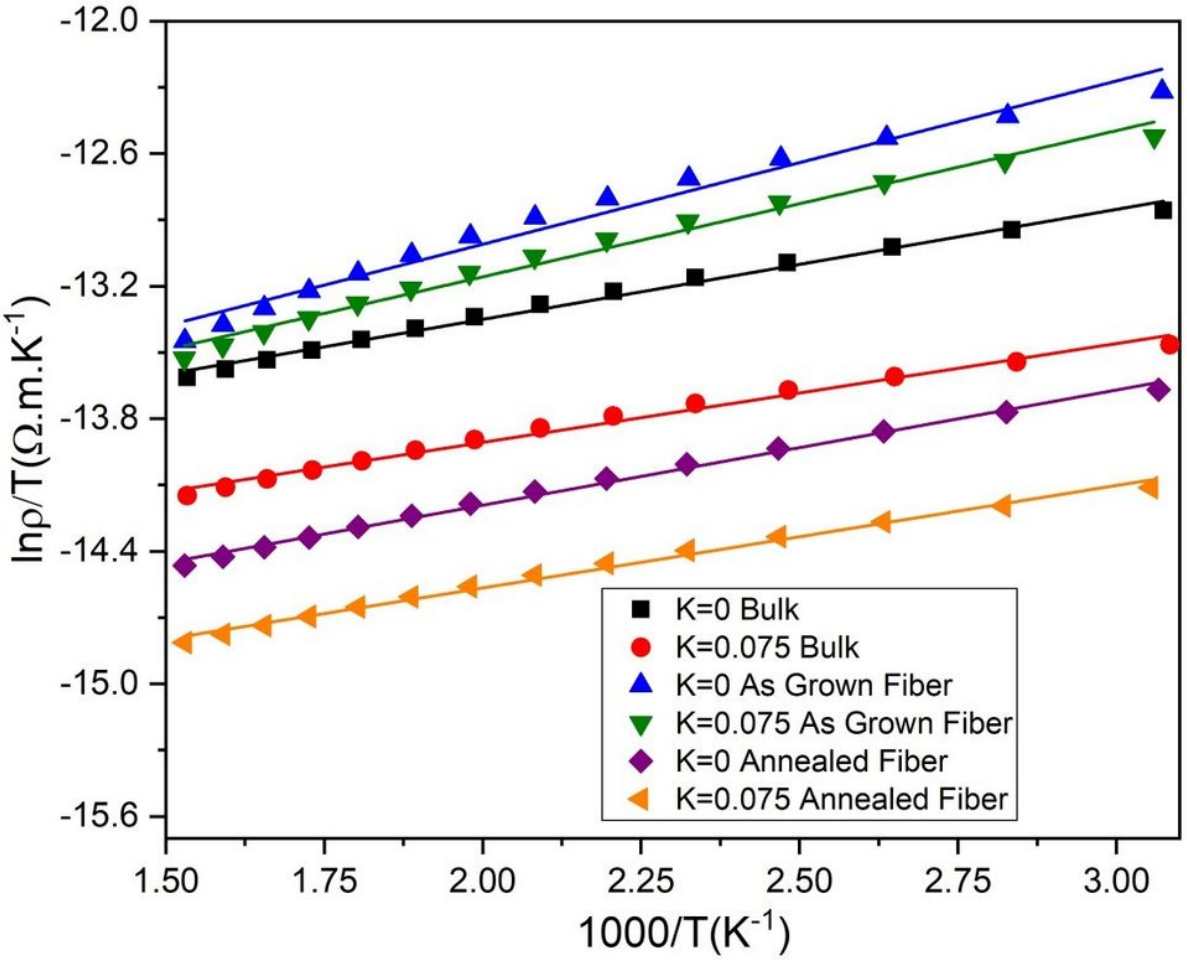

Figure 4

ln(ρ/T) versus 1000/T graph of representative BiCa2-xKxCo2Oy samples, for x=0 and 0.075.

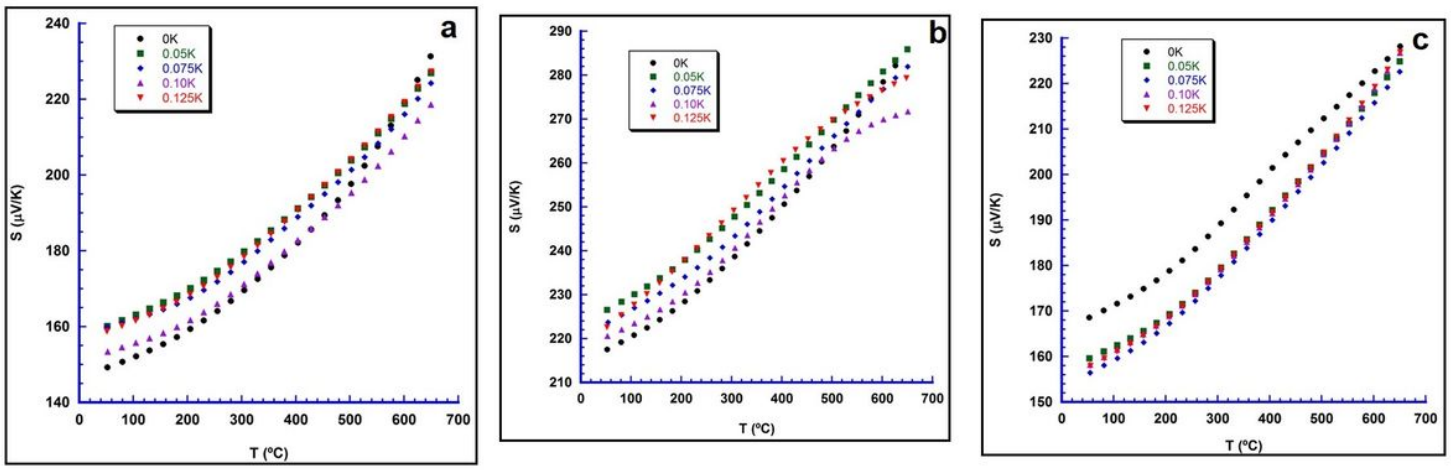

Figure 5

Seebeck coefficient variation with temperature for all BiCa2-xKxCo2Oy samples, (a) bulk, (b) as-grown, (c) annealed fibers.

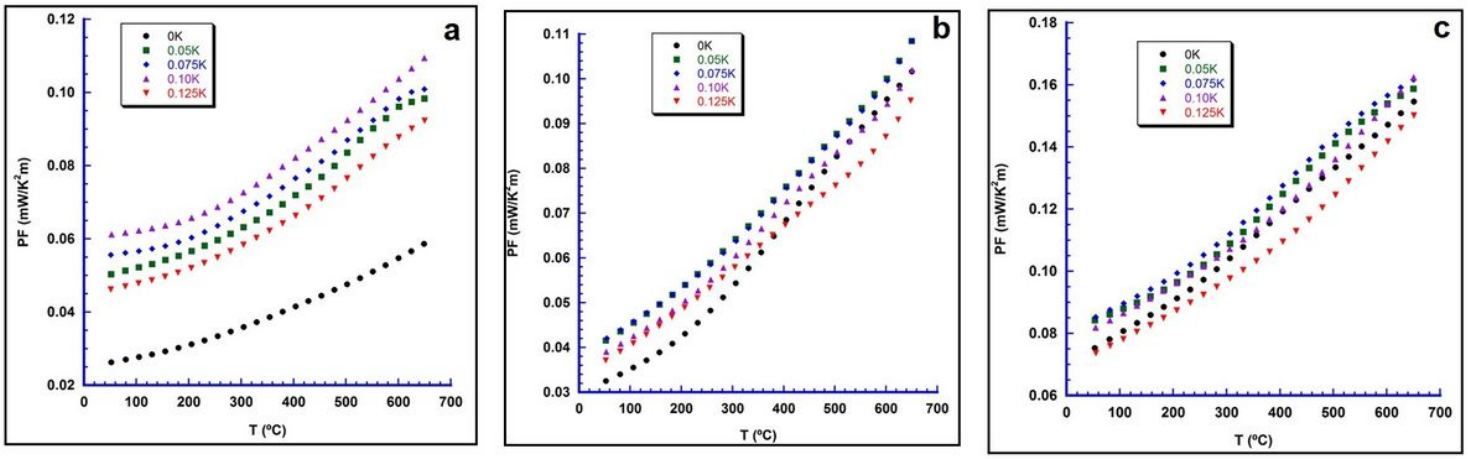

Figure 6

Power factor evolution with temperature for all BiCa2-xKxCo2Oy samples, (a) bulk, (b) as-grown, (c) annealed fibers.